Journal of Mathematical Biology (2023) 86:83
https://doi.org/10.1007/s00285-023-01912-w

Mathematical Biology

Exploring how ecological and epidemiological processes shape multi-host disease dynamics using global sensitivity analysis

Kalpana Hanthanan Arachchilage[1] · Mohammed Y. Hussaini[1] · N. G. Cogan[1] · Michael H. Cortez[2]

Received: 12 August 2022 / Revised: 24 December 2022 / Accepted: 31 March 2023

Abstract
We use global sensitivity analysis (specifically, Partial Rank Correlation Coefficients) to explore the roles of ecological and epidemiological processes in shaping the temporal dynamics of a parameterized SIR-type model of two host species and an environmentally transmitted pathogen. We compute the sensitivities of disease prevalence in each host species to model parameters. Sensitivity rankings are calculated, interpreted biologically, and contrasted for cases where the pathogen is introduced into a disease-free community and cases where a second host species is introduced into an endemic single-host community. In some cases the magnitudes and dynamics of the sensitivities can be predicted only by knowing the host species' characteristics (i.e., their competitive abilities and disease competence) whereas in other cases they can be predicted by factors independent of the species' characteristics (specifically, intraspecific versus interspecific processes or a species' roles of invader versus resident). For example, when a pathogen is initially introduced into a disease-free community, disease prevalence in both hosts is more sensitive to the burst size of the first host than the second host. In comparison, disease prevalence in each host is more sensitive to its own infection rate than the infection rate of the other host species. In total, this study illustrates that global sensitivity analysis can provide useful insight into how ecological and epidemiological processes shape disease dynamics and how those effects vary across time and system conditions. Our results show that sensitivity analysis can provide quantification and direction when exploring biological hypotheses.

Keywords Global sensitivity analysis · Dilution effect · Partial rank correlation coefficient · Environmental transmission · Daphnia

✉ Michael H. Cortez
mcortez@fsu.edu

[1] Department of Mathematics, Florida State University, Tallahassee, Fl 32306, USA

[2] Department of Biological Science, Florida State University, Tallahassee, Fl 32306, USA

Published online: 25 April 2023

Mathematics Subject Classification 37N25

1 Introduction

Many empirical studies have shown that the absence or presence of a second host species can increase or decrease levels of disease in a focal host species (Dizney and Ruedas 2009; Hydeman et al. 2017; Levine et al. 2017; Luis et al. 2018; Searle et al. 2016; Telfer et al. 2005; Zimmermann et al. 2017). This empirical work is complemented by modeling studies exploring how specific processes shape disease dynamics in two-host communities (Cortez and Duffy 2021; O'Regan et al. 2015; Roberts and Heesterbeek 2018; Rudolf and Antonovics 2005; Searle et al. 2016). Combined, these studies indicate that changes in focal host disease levels depend on both ecological processes (such as intraspecific and interspecific competition between host species for resources) and epidemiological processes (such as transmission, recovery, and disease-induced mortality). For example, disease levels in a focal host often increase when the second host has high competence (i.e., a high ability to transmit the disease), however disease levels in the focal host can instead decrease if interspecific competition between the host species is sufficiently strong (Cortez and Duffy 2021; O'Regan et al. 2015; Searle et al. 2016). In combination with empirical and theoretical work on communities with more than two host species (Cortez 2021; Dobson 2004; Faust et al. 2017; Joseph et al. 2013; Mihaljevic et al. 2014; Roche et al. 2012), this suggests that the effects of host species richness of disease dynamics are likely to be context-dependent and depend on the specific characteristics of the species present in the community (Halliday et al. 2020; LoGiudice et al. 2008; Randolph and Dobson 2012; Rohr et al. 2020). This study uses global sensitivity analysis to investigate the roles of ecological and epidemiological processes in shaping the temporal dynamics of a two-host epidemiological model.

The existing body of theory on multi-host communities has been fruitful in identifying some of the ways in which ecological and epidemiological processes shape disease-dynamics in multi-host communities. However, a key limitation of nearly every study is that they focus on asymptotic regimes of the models. In particular, many studies (e.g., Dobson 2004; O'Regan et al. 2015; Roberts and Heesterbeek 2018) focus on the pathogen basic reproduction number ($\mathcal{R}_0$), which is a measure of how fast the density or proportion of infected hosts in a population will increase in the limit where the pathogen is rare. Many other studies (e.g., Cortez and Duffy 2021; Cortez 2021; Roberts and Heesterbeek 2018; Rudolf and Antonovics 2005) focus on the density or the proportion of infected individuals in a focal host at equilibrium; these studies focus on disease dynamics in the limit where time is unbounded ($t \to \infty$). Importantly, these metrics can disagree (Cortez and Duffy 2021; Roche et al. 2012; Roberts and Heesterbeek 2018). For example, increased transmission by a second host can increase $\mathcal{R}_0$ while also decreasing the proportion of infected individuals at equilibrium (Cortez and Duffy 2021). The disagreement between metrics implies that the effects of at least one ecological or epidemiological process must differ in sign or magnitude between the two asymptotic regimes. Unfortunately, because current theory only focuses on asymptotic regimes of multi-host models, it is limited in its ability to predict when

and why the effects of specific ecological or evolutionary processes change over time. Thus, new theory is needed to help explain the different ways in which ecological and epidemiological processes shape disease dynamics over different time scales.

From a mathematical perspective, understanding the mechanisms or characteristics that have the most influence on specific outcomes (such as the proportion of infected individuals or other measures of disease dynamics) requires insight into the roles of specific parameters within a predictive model—for which sensitivity analysis is precisely designed. In this regard we can interpret a deterministic model with uncertain parameter inputs as a form of stochasticity and quantify how uncertainty in the parameters propagates through the model and affects model dynamics.

The ingredients for sensitivity analysis are:

- Input parameters (γ_i)—these may be considered as stochastic parameters with a given distribution.
- A model—some relationship between input parameters and an output. Generally we consider a system of differential equations

$$\begin{aligned} \frac{d\vec{y}}{dt} &= F(t, \vec{y}; \vec{\gamma}) \\ \vec{y}(0) &= \vec{y}_0 \end{aligned}$$

  where $\vec{y}$ is a vector of state variables, $\vec{\gamma}$ is the vector of parameters, and $\vec{y}_0$ are the initial conditions of the system.
- Quantities of Interest (QoIs; Q_i) that are functions of the state variables and model parameters,

$$Q_i = f(\vec{y}, \vec{q}).$$

In total, sensitivity analysis assesses and quantifies the relationship between individual input parameters (q_i) and the quantities of interest (QoIs; Q_i). This in turn allows one to identify influential parameters and how input perturbations affect output uncertainty.

There are a variety of sensitivity measures that have been introduced. One measure is local sensitivity, which yields a linear relationship between a parameter, γ_i, and a QoI, Q_j, via the derivative, $\frac{\partial Q_j}{\partial \gamma_i}(\vec{\bar{q}})$. This type of sensitivity analysis is referred to as 'local' in the sense that one parameter is varied at a time. Other widely used 'global' measures (which simultaneously vary multiple parameters) include Partial Rank Correlation Coefficient, Sobol' measures, importance measures and screening methods (Hanthanan Arachchilage and Hussaini 2021; Jansen 1999; Jarrett et al. 2017a; Marino et al. 2008; Salelli et al. 2004; Saltelli et al. 2019; Sobol 2001). Global approaches rely on quantifying the relationship between parameter and the QoI based on statistical relationships. They tend to be computationally expensive which is a major difficulty, especially as the number of evaluations increases with the dimensionality of the problem of interest. However, the benefit of global methods is that they can rank the parameters in terms of the magnitudes of their effects while varying all parameters simultaneously. This lowers the chance that the estimated sensitivity indices miss specific contours of the QoI as the parameter landscape changes.

We note that all sensitivity measures depend on where in parameter space we are evaluating the model. Therefore, any rankings of the parameters in terms of the magnitudes of their effects on quantities of interest depends on the location in parameter space. Additionally, local analysis almost always misses important aspects of sensitivity (Saltelli et al. 2019) and a 'global' method, where all parameters are varied simultaneous, is preferred (Salelli et al. 2004; Saltelli et al. 2019).

We use Partial Rank Correlation Coefficients (PRCC) (Marino et al. 2008) to quantify the sensitivity analysis. We use PRCC because relationships between parameters and QoIs can be nonlinear and PRCC extends the method to nonlinear relations between parameters and QoIs by focusing on ranked-transformed data. Specifically, PRCC uses rank transformation to transform (potentially nonlinear) monotonic relationships into linear relationships. In the context of noisy observations, where the relationship is not strictly monotonic, more robust conclusions can be made for relationships whose rank transform is approximately linear.

In this manuscript, we use global sensitivity analysis to explore how ecological and epidemiological processes shape the temporal dynamics of a two-host, one pathogen community. The correlation between the parameters and the QoI provides insight into the relationship between biological processes (as reflected in parameter values) and specific outcome measures. In particular a strong, positive correlation implies that small increases in the parameter value lead to qualitatively large changes in the QoI. We use this analysis to identify when and why the magnitudes and signs of the effects of specific ecological and epidemiological parameters on disease dynamics change over time. This in turn yields insight into how the corresponding ecological and epidemiological processes shape disease dynamics, and how those effects depend on the roles and identities of host species. In the following, we define the mathematical model, first developed in Searle et al. (2016), and the biological questions we address. The results section builds intuition using local sensitivities at equilibrium and then analyzes the qualitative and quantitative dynamics of the PRCC indices in multiple scenarios.

2 Mathematical model

The focal SI-type model describes the dynamics of two-host species and an environmentally transmitted pathogen. In the model, infected individuals release infectious propagules (spores) into the environment when they die and susceptible individuals become infected when they come in contact with the spores. The model was used previously (Searle et al. 2016) to model a laboratory system made up of two water flea species (*Daphnia dentifera* and *D. lumholtzi*) and a shared fungal pathogen (*Metschnikowia bicuspidata*). To match the biology of the empirical system, the model assumes individuals cannot recover from infection (meaning infection is always lethal), infected individuals release spores only when they die, and individuals in both species contribute to and are exposed to the same pool of spores because they share the same habitat.

The dynamics of the densities of susceptible (S_i) and infected (I_i) individuals in each population and the density of spores (P) are defined by a system of ordinary

differential equations:

$$\frac{dS_1}{dt} = \overbrace{r_1(S_1 + c_1 I_1)\left(1 - \alpha_{11}\left[(S_1 + I_1 e_{11}) + \alpha_{12}(S_2 + I_2 e_{12})\right]\right)}^{\text{reproduction}} - \overbrace{p_1 f_{S1} S_1 P}^{\text{infection}} - \overbrace{\delta S_1}^{\text{destructive sampling}} \tag{1}$$

$$\frac{dS_2}{dt} = \overbrace{r_2(S_2 + c_2 I_2)\left(1 - \alpha_{22}\left[(S_2 + I_2 e_{22}) + \alpha_{21}(S_1 + I_1 e_{21})\right]\right)}^{\text{reproduction}} - \overbrace{p_2 f_{S2} S_2 P}^{\text{infection}} - \overbrace{\delta S_2}^{\text{destructive sampling}} \tag{2}$$

$$\frac{dI_1}{dt} = \overbrace{f_{S1} p_1 P S_1}^{\text{infection}} - \overbrace{\delta I_1}^{\text{destructive sampling}} - \overbrace{m_1 I_1}^{\text{disease-induced mortality}} \tag{3}$$

$$\frac{dI_2}{dt} = \overbrace{f_{S2} p_2 P S_2}^{\text{infection}} - \overbrace{\delta I_2}^{\text{destructive sampling}} - \overbrace{m_2 I_2}^{\text{disease-induced mortality}} \tag{4}$$

$$\frac{dP}{dt} = \overbrace{\chi_1 m_1 I_1 + \chi_2 m_2 I_2}^{\text{release upon host death}} - \overbrace{(f_{S1} S_1 + f_{S2} S_2 + f_{I1} I_1 + f_{I2} I_2) P}^{\text{uptake}} - \overbrace{\mu P}^{\text{degradation}} - \overbrace{\delta P}^{\text{destructive sampling}} \tag{5}$$

The definitions for all variables and parameters are shown in Table 1. Throughout, we refer to parameters affecting reproduction and competition as ecological parameters ($r_i, c_i, \alpha_{ij}, e_{ij}, \delta$) and all other parameters as epidemiological parameters ($f_{S_i}, p_i, m_i, \chi_i, \mu$). This distinction facilitates the interpretation of the results, but we note that some parameters could be classified in both categories. For example, the filtering rates, f_{S_i} and f_{I_i}, affect both the uptake of infection propagules (an epidemiological process) and uptake of resources (an ecological process).

The terms in Eqs. (1) and (2) define for each species (in order) the total reproduction rates, infection rates, and rates of mortality due to destructive sampling. For host species i, r_i and $r_i c_i$ are the maximum exponential growth rates of susceptible and infected individuals, respectively; α_{ii} is the intraspecific competition parameter for susceptible individuals; α_{ij} is the relative effect of interspecific competition of species j on species i; and e_{ij} is the competitive effect of infected individuals of species j relative to the competitive effect of susceptible individuals of species j. When written in the traditional Lotka-Volterra form, the intraspecific competition coefficient for susceptible individuals for host i is α_{ii}, the intraspecific competition coefficient for infected individuals of host i is $\alpha_{ii} e_{ii}$, and the analogous interspecific competition coefficients are $\alpha_{ii}\alpha_{ij}$ and $\alpha_{ii}\alpha_{ij} e_{ij}$. The infection rates are the product of the per

Table 1 Definitions and nominal values of model parameters and variables

	Definition	Nominal value	Units
Variables			
S_i	Susceptible density for species i	Variable	Indiv./L
I_i	Infected density for species i	Variable	Indiv./L
N_i	Total density for species i	Variable	Indiv./L
Y_i	Proportion infected for species i	Variable	Unitless
P	Spore density	Variable	Spore/L
Ecological parameters			
r_1	Exponential growth rate of host 1	0.206	1/day
r_2	Exponential growth rate of host 2	0.246	1/day
c_1, c_2	proportional reduction in growth rate for I_i	0.75	Unitless
α_{11}	Intraspecific competition coefficient for host 1	1/97.5	1/indiv
α_{22}	Intraspecific competition coefficient for host 2	1/12.8	1/indiv
α_{12}	Interspecific competition coefficient for effect of host 2 on 1	2.63	Unitless
α_{21}	Interspecific competition coefficient for effect of host 1 on 2	0.01	Unitless
e_{ij}	Reduction in competitive ability of infected individuals	1	Unitless
δ	Average removal rate due to destructive sampling	0.013	1/day
Epidemiological parameters			
p_1	Per spore probability of infection for host 1	1.45×10^{-5}	1/spore
p_2	Per spore probability of infection for host 2	4.87×10^{-5}	1/spore
f_{S1}	Filtering rate for susceptible individuals of host 1	0.0348	1/L/day
f_{S2}	Filtering rate for susceptible individuals of host 2	0.0361	1/L/day
f_{I1}	Filtering rate for infected individuals of host 1	0.0186	1/L/day
f_{I2}	Filtering rate for infected individuals of host 2	0.0171	1/L/day
m_1, m_2	Disease induced mortality rate	0.05	1/day
χ_1	Spore burst size for host 1	120,000	spore/indiv
χ_2	Spore burst size for host 2	124,000	spore/indiv
μ	Spore degradation rate	0.5	1/day

All parameter estimates are taken from Searle et al. (2016)

spore probability of infection (p_i), the filtering rate of susceptible individuals (f_{S_i}), and the densities of susceptible individuals and spores.

The terms in Eqs. (3) and (4) define for each species, the rates of infection ($f_{Si}\, p_i\, P S_i$) and mortality due to destructive sampling (δI_i) and infection ($m_i I_i$). In Eq. (5), the terms define rates of release of spores by infected individuals when they die ($\chi_i m_i I_i$), uptake of spores by susceptible ($f_{S_i} S_i P$) and infected ($f_{I_i} I_i P$) individuals in each population, and loss of spores due to degradation ($-\mu P$) and destructive sampling (δP).

The quantities of interest (QoIs) in this study are the proportion of infected individuals in each population (i.e., *infection prevalence*), defined by $Y_i = I_i/N_i$ where the total density of each population is $N_i = S_i + I_i$. It is useful to write down the system

of equations for the dynamics of the total density and infection prevalence for each population,

$$\frac{dN_i}{dt} = r_i N_i(1 - Y_i + c_i Y_i)\left(1 - \alpha_{ii}\left[(1 - Y_i)N_i + e_{ii} Y_i N_i + \alpha_{ij} N_j (1 - Y_j + e_{ij} Y_j)\right]\right) - \delta N_i - m_i Y_i N_i \tag{6}$$

$$\frac{dY_i}{dt} = f_{S_i} p_i (1 - Y_i) P - (\delta + m_i) Y_i - \frac{Y_i}{N_i}\frac{dN_i}{dt} \tag{7}$$

$$\frac{dP}{dt} = \sum_j \chi_j m_j Y_j N_j - \sum_j \left[f_{S_j}(1 - Y_j) + f_{I_j} Y_j\right] N_j P - \mu P - \delta P \tag{8}$$

The terms in Eq. (6) define how the total density of each population changes due to reproduction and mortality. The terms in Eq. (7) define how the disease prevalence increases due to transmission, decreases due to mortality, and changes as the density of susceptible individuals increases or decreases. Equation (8) is identical to Eq. (5).

The nominal values for all parameters are shown in Table 1 and were taken from Searle et al. (2016). Briefly, the parameters were estimated in Searle et al. (2016) in the following way. The epidemiological parameter values (e.g., probabilities of infection, spore burst sizes, and mortality rates) were estimated using individual-level experiments where individual daphniids were exposed to fungal spores and disease-related characteristics were measured. The ecological parameter values (exponential growth rates and competition coefficients) were estimated by fitting Eqs. (1) and (2) to time series data where one or both host species were present and the pathogen was absent. The value for the spore degradation rate ($\mu = 0.5$) was taken from a range of values ($0 \leq \mu \leq 0.75$) within which there was qualitative agreement between the model predictions and experiments where both host species were present with the pathogen.

The models have a unique coexistence equilibrium where all state variables are positive. We refer to this equilibrium as the endemic equilibrium and denote its values using S_i^*, I_i^*, N_i^*, Y_i^*, and P^*.

3 Problem statement and cases

The goal of this study is to use sensitivity analysis to explore how ecological and epidemiological processes shape the temporal dynamics of disease prevalence in model (1)–(5). Our metric for computing global sensitivities is Partial Rank Correlation Coefficients (PRCC) (Blower and Dowlatabadi 1994; Hamby 1995; Hanthanan Arachchilage and Hussaini 2021; Jarrett et al. 2017b; Marino et al. 2008; Wentworth et al. 2016). PRCC quantifies how the variations in the model parameters affect the values of the quantities of interest (QoIs); an overview of the method is provided in Appendix A. We note that PRCC requires a monotonic relationship between the parameter and QoI. The monotonicity condition was satisfied by all of the parameters and QoIs considered in this study.

We focus on answering the following questions.

1. How do the magnitudes and signs of the sensitivities of host prevalence to model parameters change over time?
2. When the pathogen is introduced into a disease-free two-host community, how do the temporal patterns depend on the identities of the host species?
3. When a second host species is introduced into a single-host community with an endemic pathogen, how do the temporal patterns depend on which host species is the resident and which is the invader?

We answer these questions by applying sensitivity analysis to simulations of the model in three cases:

Case 1: A moderate amount of spores is added to a disease-free two-host community at equilibrium.
Case 2: Host 2 is introduced at low densities to the single-host endemic equilibrium for host 1. Here, host 1 is the resident and host 2 is invader.
Case 3: Host 1 is introduced at low densities to the single-host endemic equilibrium for host 2. Here, host 2 is the resident and host 1 is invader.

Case 1 identifies if and how the specific characteristics of each host species affect disease dynamics when the pathogen is introduced into the community. Comparing Cases 2 and 3 identifies how the identities of the resident and invader hosts influence disease dynamics.

Specific details about the simulations are the following. In case 1, the initial conditions for the simulations are

$$S_1(0) = \frac{r_1 - \delta}{r_1\alpha_{11}(1 - \alpha_{12}\alpha_{21})} - \frac{(r_2 - \delta)\alpha_{12}}{r_2\alpha_{22}(1 - \alpha_{12}\alpha_{21})} \tag{9}$$

$$S_2(0) = \frac{r_2 - \delta}{r_2\alpha_{22}(1 - \alpha_{12}\alpha_{21})} - \frac{(r_1 - \delta)\alpha_{21}}{r_1\alpha_{11}(1 - \alpha_{12}\alpha_{21})}. \tag{10}$$

with $I_1(0) = 0$, $I_2(0) = 0$, and $P(0) = 25000$. In cases 2 and 3, the system is initiated with nonzero densities for the resident host and spores and the model is run for 2000 days to ensure convergence to the single-host endemic equilibrium. Day 0 is defined as the day the invading host is introduced. The invading host is introduced at 1% of the susceptible density of the resident host (e.g., if host 2 is the invader, then $S_2(0) = 0.01 \times S_1(0)$).

4 Results

The results are organized as follows. Section 4.1 builds intuition about the expected signs of the PRCC sensitivity indices using the differential equations in the model (Sect. 4.1.1) and local sensitivities evaluated at the two-host endemic equilibrium (Sect. 4.1.2). Section 4.2 compares those expected signs with the signs of the PRCC sensitivities computed for Cases 1–3 and focuses on explaining when and why the signs of the global sensitivities agree and disagree with the expected signs. Section 4.3 focuses on the magnitudes of the PRCC sensitivities. That section explores the quantitative dynamics of the PRCC sensitivities and explains the biological insight that is

gained by analyzing the temporal dynamics in Case 1 (Sect. 4.3.1) and by comparing temporal dynamics of Cases 2 and 3 (Sect. 4.3.2).

4.1 Building intuition about the expected signs of the global sensitivities

4.1.1 Expected signs based on model equations

One way to build intuition about the signs of the global sensitivities is to compute the partial derivatives of the growth rates for disease prevalence (dY_i/dt) and spore density (dP/dt) with respect to the model parameters. The mathematical reasoning for considering how parameter values affect the derivative of a state variable is the following. For one-dimensional systems, changes in parameter values have effects of the same sign on the state variable and its derivative at all points in time and at equilibrium. Specifically, let $Q_{\gamma_1}(t)$ denote the solution to the autonomous ODE $dQ/dt = F(Q, \gamma)$ with parameter γ and initial condition $Q(0) = Q_0$. If F is an increasing function of γ, i.e., $\partial F/\partial\gamma > 0$, then $Q_{\gamma_1}(t) > Q_{\gamma_2}(t)$ for all $\gamma_1 > \gamma_2$ for all time and if F is a decreasing function of γ, i.e., $\partial F/\partial\gamma < 0$, then $Q_{\gamma_1}(t) < Q_{\gamma_2}(t)$ for all $\gamma_1 > \gamma_2$ for all time. In addition, at a stable equilibrium, Q^*, of the ODE, which must satisfy $\partial F/\partial Q|_{Q^*} < 0$, we get that $\partial Q^*/\partial\gamma|_{N^*} = -(\partial F/\partial\gamma)/(\partial F/\partial Q)|_{Q^*}$, which has the same sign as $\partial F/\partial\gamma$. For higher dimension systems, changes in parameter values have effects of the same sign on the state variable and its derivative over sufficiently short time scales. However, over longer time scales and at equilibrium, the effects can be of opposite signs due to the feedbacks between all state variables. Thus, the effects of changes in parameter values on the derivative of a state variable yield insight into how changes in parameter values affect the value of a state variable over short time scales and they can, but do not always, yield insight into how changes in parameter values affect the value of a state variable over long time scales.

Based on the above, the intuition is that disease prevalence in host i ($Y_i = I_i/N_i$) will increase and decrease with variation in a parameter based on whether the parameter causes the growth rates of disease prevalence and spore density to increase or decrease, respectively. In particular, one might expect that prevalence in host i and a parameter γ are (a) positively correlated if the partial derivatives of dY_i/dt or dP/dt with respect to γ are positive (i.e, $[\partial/\partial\gamma][dY_i/dt] > 0$ or $[\partial/\partial\gamma][dP/dt] > 0$), (b) negatively correlated if the partial derivatives of dY_i/dt or dP/dt with respect to γ are negative (i.e, $[\partial/\partial\gamma][dY_1/dt] < 0$ or $[\partial/\partial\gamma][dP/dt] < 0$), and (c) uncorrelated if dY_i/dt and dP/dt do not depend on γ (i.e, $[\partial/\partial\gamma][dY_1/dt] = 0$ and $[\partial/\partial\gamma][dP/dt] = 0$).

The signs of the derivatives of the growth rates are summarized in the columns labeled "Model Eqns." in Table 2. We note two issues with the intuition gained from this approach. First, in general, this approach is unlikely to predict the signs of the global sensitivities in all cases because it ignores feedbacks between the variables. For example, dY_i/dt does not depend on probability of infection for the other host species ($p_j, i \neq j$), but the value of p_j will have an indirect effect on the magnitude of dY_i/dt because the differential equations are coupled. Second, for some parameters the signs of the derivatives of the dY_i/dt and dP/dt equations differ, which makes it difficult to predict the sign of the correlation between prevalence and the parameter.

For example, dY_1/dt is an increasing function of the host filtering rate (f_{S_1}) whereas dP/dt is a decreasing function.

4.1.2 Signs of local sensitivities computed at equilibrium

Another way to build intuition about the signs of global sensitivities is to compute local sensitivities at equilibrium. While global sensitivities are often better to use than local sensitivities (as discussed in the Introduction), we compute the local sensitivities at equilibrium for two reasons. First, the local sensitivity of the equilibrium value of a QoI, Q^*, to a parameter, γ, can be computed analytically via the partial derivatives $\partial Q^*/\partial\gamma$; see appendix B.1 for details. In addition, Cortez and Duffy (2021) and Cortez (2021) analyzed generalized versions of models (1)-5) and (6)–(7) and showed that the analytical formulas can be interpreted in terms of indirect feedbacks between variables. Thus, the local sensitivities at equilibrium allow us to connect biological mechanism with computed signs of the local sensitivities. Second, when the parameters are set to the nominal values, the simulations for Cases 1, 2, and 3 converge to the (unique) endemic equilibrium used to compute the local sensitivities. Combined, this suggests that insight gained about the mechanisms determining the signs of the local sensitivities at equilibrium may also yield insight into the mechanisms determining the signs of the global sensitivities at sufficiently large time scales. Moreover, if the signs of the local sensitivities at equilibrium and the signs of the global sensitivities at shorter time scales agree, then the mechanistic insight gained from the local sensitivities provides a good starting point for understanding the mechanisms driving the signs of the global sensitivities at short time scales. In total, studying the local sensitivities at equilibrium is useful because they provide a good starting point when trying to connect biological mechanism with observed patterns in the global sensitivities.

The signs of the local sensitivities for the nominal parameter values are given in the columns labeled "Eq. Local Sensitivity" in Table 2; see appendix B.2 for details about each individual parameter. The overall patterns are that infectious prevalence in either host increases with higher host reproduction rates (larger r_i and c_i and smaller α_{ij} and e_{ij}), higher rates of infection (larger p_i and f_{S_i}), higher spore release rates (larger χ_i and m_i), and lower loss rates of spores (smaller f_{I_i}, μ, and δ). The intuition is that higher host densities, higher transmission rates, and greater spore density lead to greater contact between susceptible individuals and spores, which leads to more infections and higher prevalence. The only exception is that the local sensitivity for infection prevalence in host 2 (I_2/N_2) is negative for its own mortality rate (m_2). The reason is that host 2 density is very low and while increased mortality leads to greater release rates of spores, it also reduces the population size of the second host, which leads to fewer infected individuals of host 2.

4.1.3 Comparisons and limitations of predicted signs

The intuition gained from the previous two approaches agrees for some parameters and disagrees for others; see appendix B.3 for discussions about why disagreement occurs for specific parameters. Agreement and disagreement both provide useful biological insight because they identify ecological and epidemiological processes whose

Table 2 Computed signs of global and local sensitivities

Parameter	Quantity of Interest 1, $Y_1 = I_1/N_1$					Quantity of Interest 2, $Y_2 = I_2/N_2$				
	Model Eqns.*	Case 1 $t > 0$	Case 2 $t > 0$	Case 3 $t > 0$	LSA Eq.*	Model Eqns.*	Case 1 $t > 0$	Case 2 $t > 0$	Case 3 $t > 0$	LSA Eq.*
Ecological										
r_1	−	− ↑ +	+ ↕ +	− ↕ +	+		− ↑ +	+ ↕ +	+ ↕ +	+
r_2		+↑ +	+↕ +	+ ↕ +	+	−	+ ↑ +	− ↕ +	+ ↕ +	+
C_1	−	− ↕ +	+ ↕ +	− ↕ +	+	−	− ↕ +	+ ↕ +	+ ↕ +	+
C_2		+ ↑ +	− ↑ +	+ ↕ +	+		− ↑ +	− ↕ +	+ ↕ +	+
α_{11}	+	+ ↓ −	− ↑ −	+ ↕ −	−		+ ↓ −	− ↕ −	− ↕ −	−
α_{12}	+	+ ↓ −	+ ↕ −	+ ↕ −	−		+ ↓ −	+ ↕ −	+ ↕ −	−
α_{21}		− ↕ −	+ ↓ −	− ↕ −	−	+	− ↕ −	+ ↕ −	− ↕ −	−
α_{22}		− ↕ −	− ↓ −	− ↕ −	−	+	− ↕ −	+ ↕ −	− ↕ −	−
e_{ij}	+	+ ↓ −	− ↕ −	− ↕ −	−	+	+ ↓ −	− ↕ −	− ↑ −	−
δ	−	− ↓ −	− ↓ −	− ↕ −	−	−	− ↓ −	− ↓ −	− ↕ −	−
Epidemiological										
p_1	+	+ ↕ +	+ ↕ +	+ ↑ +	+		+ ↑ +	+ ↓ +	+ ↑ +	+
p_2		+ ↕ +	− ↑ +	+ ↓ +	+	+	+ ↓ +	+ ↑ +	+ ↓ +	+
f_{S_1}	+	+ ↕ +	+ ↑ +	+ ↕ +	+	−	− ↑ +	+ ↕ +	+ ↕ +	+
f_{S_2}	−	− ↕ +	− ↕ +	+ ↕ +	+	+	+ ↓ +	+ ↑ +	+ ↓ +	+
f_{I_1}	−	− ↓ −	− ↓ −	+ ↓ −	−	−	+ ↓ −	− ↓ −	+ ↓ −	−
f_{I_2}	−	− ↓ −	− ↓ −	− ↑ −	−	−	− ↓ −	− ↓ −	− ↑ −	−
m_1	+	+ ↕ +	+ ↓ +	− ↕ +	+	+	+ ↑ +	+ ↕ +	+ ↑ +	+

Table 2 continued

Parameter	Quantity of Interest 1, $Y_1 = I_1/N_1$					Quantity of Interest 2, $Y_2 = I_2/N_2$				
	Model Eqns.*	Case 1 $t > 0$	Case 2 $t > 0$	Case 3 $t > 0$	LSA Eq.*	Model Eqns.*	Case 1 $t > 0$	Case 2 $t > 0$	Case 3 $t > 0$	LSA Eq.*
m_2	+	+ ↕ +	− ↑ +	+ ↓ +	+	+	− ↕ −	− ↓ −	+ ↕ −	−
χ_1	+	+ ↑ +	+ ↓ +	+ ↑ +	+	+	+ ↑ +	+ ↓ +	+ ↑ +	+
χ_2	+	+ ↕ +	+ ↑ +	+ ↓ +	+	+	+ ↕ +	+ ↑ +	+ ↓ +	+
μ	−	− ↓ −	− ↓ −	− ↑ −	−	−	− ↓ −	− ↓ −	− ↑ −	−

Plus (+) and minus (−) signs mean positive and negative values, respectively. The ordering of the signs indicates how the sign of the global sensitivity changes as time increases from zero (left sign) to infinity (right sign). Up arrows (↑) and down arrows (↓) mean that the global sensitivity value changes monotonically as time increases. Up-down arrows (↕) mean that the global sensitivity value changes in a non-monotonic way

∗ Signs based on the derivatives of the model equations (Model Eqns.) and the local sensitivities evaluated at the two-host endemic equilibrium (LSA Eq.); see text for details. Plus (+) and minus (−) signs mean positive and negative values, respectively. Blank entries mean that the dY_i/dt and dP/dt equations are independent of the parameter

influence on disease prevalence may or may not vary over time. Cases of agreement could suggest that the signs of the global sensitivities are the same at all points in time, which would mean that the corresponding biological processes have effects of the same sign on infection prevalence at all time scales. Applying this logic to Table 2, we predict that infection probabilities (p_i) and spore burst sizes (χ_i) have positive effects at all time scales and filtering by infected individuals (f_{I_i}), spore degradation (μ), and destructive sampling (δ) have negative effects at all time scales. In comparison, cases of disagreement suggest that the signs of the global sensitivities are likely to differ over time, which would mean that the corresponding biological processes can have effects of different signs on infection prevalence at different points in time. Applying this to Table 2, we predict that host reproduction (r_i, c_i), host competition (α_{ij}, e_{ij}), host mortality (m_i), and filtering by susceptible individuals (f_{S_i}) could have positive and negative effects on infection prevalence.

We note three things about the predictions. First, in general, the predictions from the two approaches differ because the local sensitivities account for all direct and indirect effects between the model variables whereas the derivatives of the model equations only account for direct effects. Second, as explained above, the predictions from each approach have the potential to identify the mechanisms determining the signs of the global sensitivities. However, an important limitation is that local sensitivities at equilibrium and the derivatives of the model equations do not account for variation in the initial state of the system, i.e., the initial conditions of the model. In particular, the initial conditions in Cases 1–3 are defined by equilibria of the system, whose locations in phase space depend on the model parameters (e.g., the location of the disease-free two-host equilibrium depends on the competition coefficients α_{ij}). Thus, the signs and magnitudes of the global sensitivities could be influenced by the initial conditions of the system. Third, while local sensitivity accounts for feedbacks between variables, it only provides a limited exploration of parameter space and phase space. Specifically, the local sensitivity calculations only compute infinitesimal variations in one parameter at a time (and implicitly assumes the gradients stay the same throughout the entire parameter space), which provides a very limited exploration of parameter space, and they are only evaluated at the endemic equilibrium, which provides a very limited exploration of phase space. Consequently, while the local sensitivities have the potential to explain some mechanisms determining the signs of the global sensitivities (as explained above), those predictions may be inaccurate as parameters are varied over large ranges and state variables vary over time.

4.2 Analysis of temporal changes in the signs of global sensitivities

We now analyze the temporal changes in the signs of the global sensitivities for disease prevalence in each host species. We focus on parameters whose global sensitivities differ in sign at some time point from the local sensitivities at equilibrium. This helps identify the general mechanisms explaining why the effects of specific ecological and epidemiological processes on disease prevalence can differ in sign over different time scales. To avoid analyzing every parameter and to reduce length, we focus on the most sensitive parameters, which we define as the parame-

ters whose PRCC values exceed 0.6 for at least one host at some point in time (i.e, $max|PRCC(t)| \geq 0.6$). The main text focuses on parameters whose PRCC values exceed 0.75 (i.e, $max|PRCC(t)| \geq 0.75$) and we refer the reader to appendix C for discussion about the other parameters whose PRCC values exceed 0.6. The temporal dynamics for the most sensitive parameters are plotted in Figs. 1, 2, 3. Table 2 roughly summarizes the trends. In particular, for each entry in Table 2, the first symbol is the sign at $t \approx 0$, the third symbol is the sign at $t = 3000$, and the middle symbol shows whether the PRCC value increases monotonically (up arrow), decreases monotonically (down arrow) or changes in a non-monotonic way (up-down arrow).

There are three takeaways from Figs. 1, 2 and 3 and Table 2. First, in many instances there is agreement between the signs of the global sensitivities and the signs of the local sensitivities at equilibrium. Specifically, there is agreement (i) for all parameters in all cases at sufficiently large time (i.e., third symbol for each case agrees with the symbol in "LSA Eq." column); (ii) for each parameter there is agreement for all time points in at least one of the three cases (e.g., signs for r_1 agree for cases 2 and 3, but not case 1); and (iii) for a few parameters (χ_i, δ, μ) there is agreement for all time points in all three cases. These instances of agreement suggest that, for the range of variation used in the global sensitivity calculations, the signs of the global sensitivities are likely driven by the same mechanisms that explain the signs of the local sensitivities at equilibrium. For example, positive global sensitivities for χ_1 and χ_2 for δ and μ are likely due to those parameters increasing spore density, which leads to higher contact rates between susceptible individuals and spores and ultimately, more infections and higher infection prevalence. Similarly, negative global sensitivities for δ and μ are likely due to those parameters decreasing the spore densities, which ultimately leads to fewer infections and lower infection prevalence.

Second, for nearly all parameters, there exists at least one case where the signs of the global sensitivities and local sensitivities disagree for finite periods of time. This means that for almost every ecological or epidemiological process, the sign of the effect of that process on infection prevalence in one or both host species changes sign. The sign change is important biologically because it shows that most ecological and epidemiological processes can facilitate disease spread over some time scales and impede it over other time scales.

Third, the specific conditions under which the sign changes occur identify when and how nonlinear interactions between multiple processes lead to unexpected effects of a process on infection prevalence. Our numerical results show that sign changes in the most sensitive parameters occur because of how host reproduction and production of spores influence infection prevalence. Brief explanations for the sign changes for the most sensitive parameters in each case are provided below; see appendix C for additional details.

In Case 1, the sensitivities of host 1 prevalence (I_1/N_1) and host 2 prevalence (I_2/N_2) to the intraspecific competition coefficient for host 1 (α_{11}) change from positive to negative (red plus signs in Fig. 1a, b) and the sensitivities of prevalence in both host species to the filtering rate of host 1 (f_{S_1}) change from positive to negative to positive (red diamonds in Fig. 1a, b). The reason for all sign changes is that spore density is initially very low and host 2 produces more spores per infected individual than host 1. Consequently, reduced density and filtering by host 1 results in faster increases in

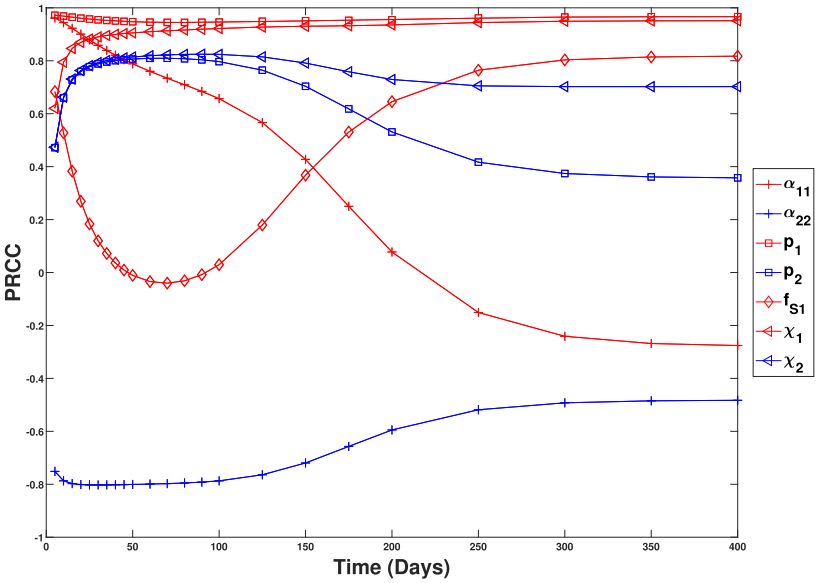

(a) Case 1 - Infection prevalence in host 1 (I_1/N_1)

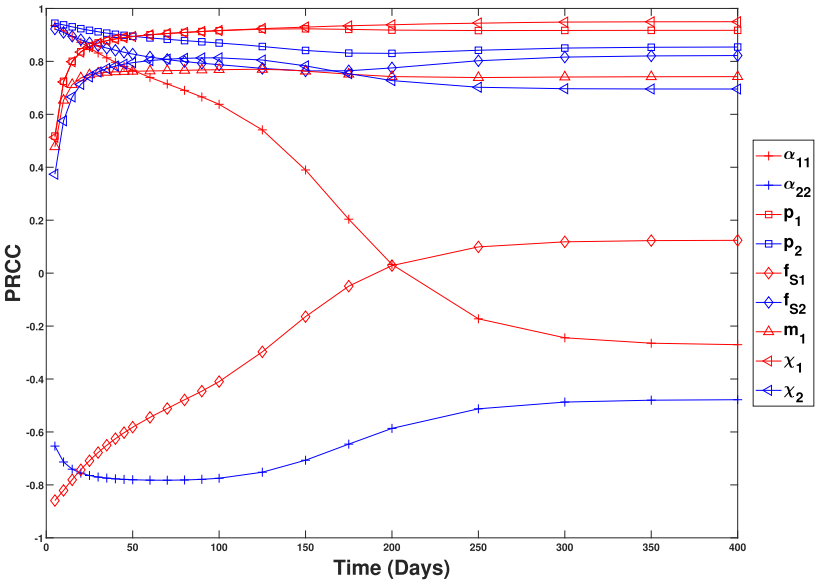

(b) Case 1 - Infection prevalence in host 2 (I_2/N_2)

Fig. 1 Temporal patterns in the global sensitivities for Case 1. In Case 1, the pathogen is introduced into the two-host community at equilibrium. Each panel shows the global sensitivities for parameters satisfying $\max(|PRCC(t)| \geq 0.75$ for (top) disease prevalence in host 1, I_1/N_1, and (bottom) disease prevalence in host 2, I_2/N_2. The specific parameter associated with each curve is given in the legend; red corresponds to parameter values for host 1 and blue corresponds to parameter values for host 2 (colour figure online)

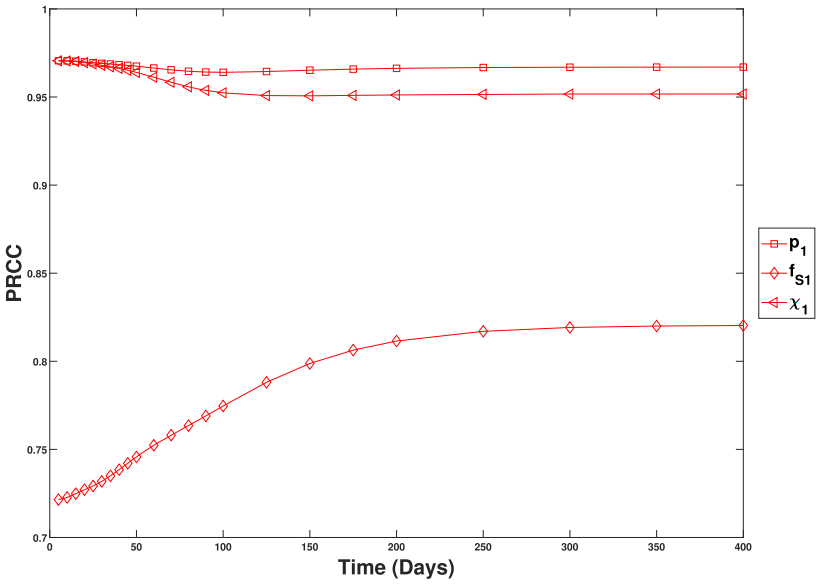

(a) Case 2 - Infection prevalence in host 1 (I_1/N_1)

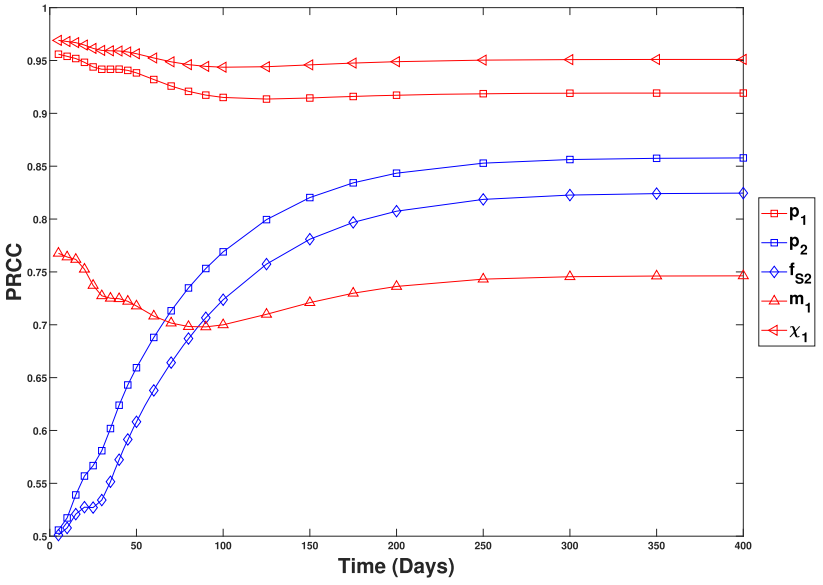

(b) Case 2 - Infection prevalence in host 2 (I_2/N_2)

Fig. 2 Temporal patterns in the global sensitivities for Case 2. In Case 2, host 2 is introduced into the endemic community made up of host 1 and the pathogen. Each panel shows the global sensitivities for parameters satisfying $\max(|PRCC(t)| \geq 0.75$ for (top) disease prevalence in host 1, I_1/N_1, and (bottom) disease prevalence in host 2, I_2/N_2. The specific parameter associated with each curve is given in the legend; red corresponds to parameter values for host 1 (the resident), blue corresponds to parameter values for host 2 (the invader), and green corresponds to parameter values for the pathogen (colour figure online)

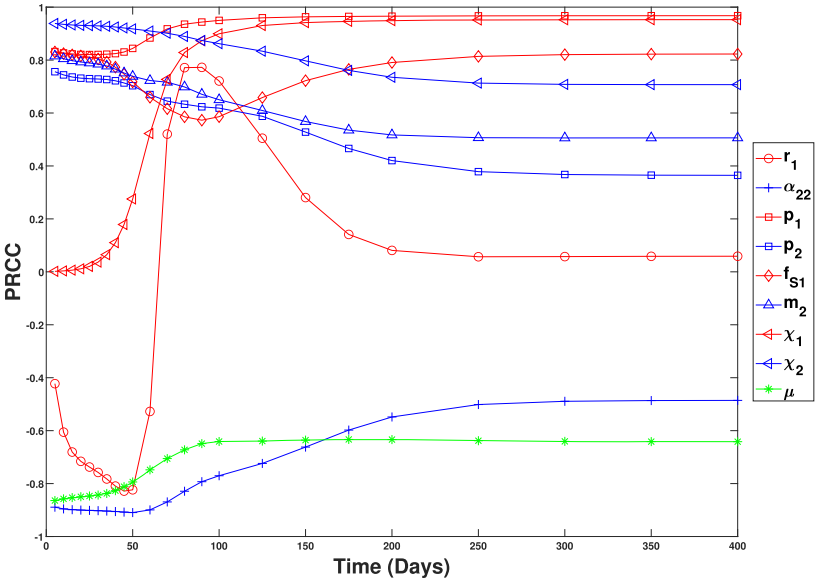

(a) Case 3 - Infection prevalence in host 1 (I_1/N_1)

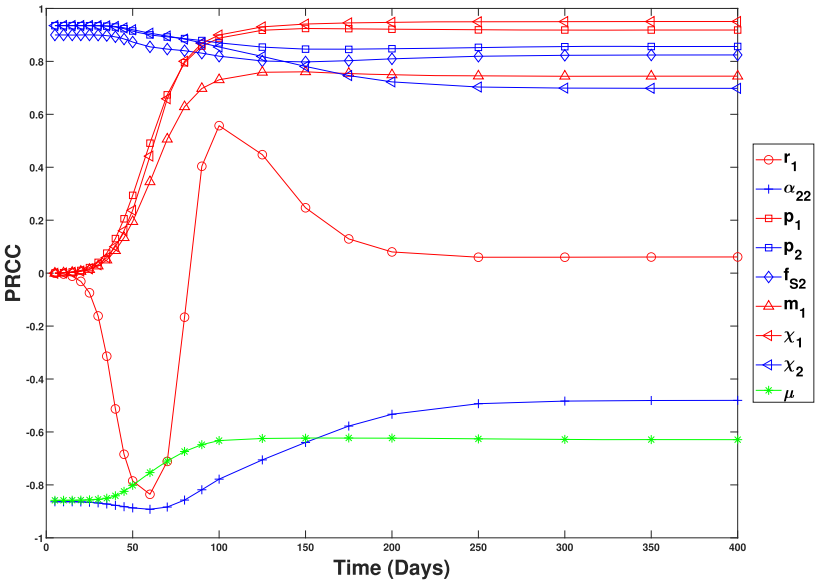

(b) Case 3 - Infection prevalence in host 2 (I_2/N_2)

Fig. 3 Temporal patterns in the global sensitivities for Case 3. In Case 3, host 1 is introduced into the endemic community made up of host 2 and the pathogen. Each panel shows the global sensitivities for parameters satisfying $\max(|PRCC(t)| \geq 0.75$ for (top) disease prevalence in host 1, I_1/N_1, and (bottom) disease prevalence in host 2, I_2/N_2. The specific parameter associated with each curve is given in the legend; red corresponds to parameter values for host 1 (the invader) and blue corresponds to parameter values for host 2 (the resident) (colour figure online)

spore density, and thus more infections in both hosts. However, later in time greater density and filtering in host 1 yields higher spore density and more infections in both hosts.

In Case 2 (Fig. 2), the signs of the global sensitivities for the most sensitive parameters do not change sign.

In Case 3, the sensitivities of host 1 prevalence (I_1/N_1) and host 2 prevalence (I_2/N_2) to the reproduction rate of host 1 (r_1) exhibit substantial change in both sign and magnitude (red circles in Fig. 3a, b). Early in time (day 0 to 75), host 1 is increasing from low densities. Increased reproduction of host 1 causes the density of susceptible individuals of host 1 to increase faster than the density of infected individuals. The sensitivity for host 1 prevalence is negative because faster growth of susceptible individuals than infected individuals necessarily causes host 1 prevalence to decrease. The sensitivity for host 2 prevalence is negative because greater host 1 density results in great uptake of spores, which decreases the infection rate for host 2 and decreases host 2 prevalence. Both global sensitivities are large in magnitude because variation in the growth rate of host 1 has a large effect on how fast host population 1 exponentially grows. Later in time (day 75–150), susceptible density of host 1 overshoots its equilibrium value (see Figure B9), which results in susceptible density of host 1 decreasing over time. This reverses the signs of the global sensitivities because greater reproduction by host 1 means there are more susceptible individuals who can subsequently become infected. As a result, increased reproduction of host 1 yields higher prevalence in host 1, and because higher host 1 prevalence yields greater spore densities, higher prevalence in host 2 as well. Both global sensitivities are large in magnitude because variation in the growth rate of host 1 has a large effect on how the rate of production of susceptible individuals (who can subsequently become infected). As the system converges to equilibrium (day 150 and later), the global sensitivities of both prevalence monotonically decrease to small positive values. The values are small in magnitude because the host growth rates have a small effect on the densities and prevalences at equilibrium. The values are positive because increased reproduction by host 1 leads to greater densities of host 1, which increases host 1 prevalence. In addition, increased host 1 prevalence yields greater spore densities, which results in increased host 2 prevalence.

4.3 Comparisons of global sensitivities across cases

Here, we compare the temporal dynamics of the PRCC sensitivity indices across the three cases in order to answer questions two and three posed in Sect. 3. The first subsection compares the temporal dynamics of the sensitivities for the two host species in Case 1. The second subsection compares the temporal dynamics for the two host species across Cases 2 and 3. We do not compare the temporal dynamics of Case 1 with those of Cases 2 and 3 because the differences in initial conditions make it unclear what biological insight can be gained. As in Sect. 4.2, we provide brief explanations for parameters whose PRCC values exceed 0.75 at some point in time (Table 3) and refer the reader to appendix D for detailed explanations of all parameters whose PRCC values exceed 0.6.

Table 3 Comparison of parameters satisfying $max|PRCC(t)| \geq 0.75$ in each case

Parameter	Case 1		Case 2		Case 3	
	QoI 1 $Y_1 = I_1/N_1$	QoI 2 $Y_2 = I_2/N_2$	QoI 1 $Y_1 = I_1/N_1$	QoI 2 $Y_2 = I_2/N_2$	QoI 1 $Y_1 = I_1/N_1$	QoI 2 $Y_2 = I_2/N_2$
r_1					✓	✓
α_{11}	✓	✓				
α_{22}	✓	✓			✓	✓
p_1	✓	✓	✓	✓	✓	✓
p_2	✓	✓		✓	✓	✓
f_{S_1}	✓	✓	✓		✓	
f_{S_2}		✓		✓		✓
m_1		✓		✓		✓
m_2					✓	
χ_1	✓	✓	✓	✓	✓	✓
χ_2	✓	✓			✓	✓
μ					✓	✓

Figures 4, 5 and 6 show the sensitivities to parameters for host species 1 (blue curves) and host species 2 (red curves) in Case 1 (circles), Case 2 (squares), and Case 3 (triangles). For Figs. 5 and 6 solid curves with filled symbols denote the resident's parameters and dashed curves with open symbols denote the invader's parameters. Our comparisons focus on identifying when the magnitudes and dynamics of the sensitivities are driven by (i) intraspecific versus interspecific processes, (ii) the species' roles of invader versus resident, or (iii) the species' identities; see below for details about each.

First, we say the magnitudes and dynamics of the sensitivities are driven by intraspecific versus interspecific processes, if the sensitivities of each quantity of interest to its own parameters are qualitatively similar and the sensitivities of each quantity of interest to the other species' parameter values are qualitatively similar. That is, the sensitivities of I_i/N_i $(i = 1, 2)$ to parameter γ_i are qualitatively similar and the sensitivities of I_i/N_i $(i = 1, 2)$ to parameter γ_j $(j \neq i)$ are qualitatively similar. Biologically, this means the effects of a biological process on disease prevalence can be predicted independent of specific characteristics (e.g., competitive ability or competence) or roles (invader vs. resident) of the two host species. This suggests that the effects of that biological process are the same in all systems, regardless of which host species are present. In Figs. 4, 5 and 6, this means blue curves in the top panel are qualitatively similar to red curves in the bottom panel and red curves in the top panel are qualitatively similar to blue curves in the bottom panel. For example, early in time in Case 1, prevalence in host i is more sensitive to its own probability of infection (p_i; intraspecific parameter) than the probability of infection of the other host (p_j, $j \neq i$; interspecific parameter) (for small t, solid blue curve above solid red curve in top panel of column 2 in Fig. 4 and solid red curve above solid blue curve in bottom panel of column 2 in Fig. 4). As another example, early in time in Case 1, prevalence

in host i is more sensitive to the other host's mortality rate (m_j, $i \neq j$; interspecific parameter) than its own mortality rate (m_i; intraspecific parameter) (for small t, solid red curve above solid blue curve in top panel of column 4 in Fig. 4 and solid blue curve above solid red curve in bottom panel of column 4 in Fig. 4).

Second, we say the magnitudes and dynamics of the sensitivities are determined by the species' roles of invader versus resident, if the sensitivities of I_1/N_1 and I_2/N_2 to the resident's parameter values are qualitatively similar and the sensitivities to the invader's parameter values are qualitatively similar. Biologically, this means the effects of the biological process on disease prevalence can be predicted solely by the species' role (invader vs. resident) and independent of the specific characteristics (e.g., competitive ability or competence) of the two host species. This suggests that the effects of that biological processes are the same in all systems, regardless of which host species is the resident or invader. In Figs. 5 and 6, this means solid curves with filled symbols are qualitatively similar and dashed curves with open symbols are qualitatively similar. For example, early in time in Cases 2 and 3, I_1/N_1 and I_2/N_2 are both more sensitive to the resident's intraspecific competition coefficient (α_{ii}) than the invader's competition coefficient. Specifically, for small t in both panels of column 2 of Fig. 6, the solid blue curve with filled squares is larger in magnitude than the dashed red curve with open squares (i.e., Case 2) and the solid red curve with filled triangles is larger in magnitude than the dashed blue curve with open triangles (i.e., Case 3).

Third, we say the magnitudes and dynamics of the sensitivities are predicted by species' identities, if the sensitivities of I_1/N_1 and I_2/N_2 to host species 1's parameter values are qualitatively similar and the sensitivities to host species 2's parameter values are qualitatively similar. Biologically, this means the effects of the biological process on disease prevalence can be predicted only when the specific characteristics of the host species are known. This suggests that the biological process can have different effects in systems where different host species are present. In Figs. 4, 5 and 6, this means blue curves in the top panel are qualitatively similar to red curves in the bottom panel and red curves in the top panel are qualitatively similar to blue curves in the bottom panel. For example, in Case 1, prevalence in both species is more sensitive to the burst size of host 1 (χ_1) than host 2 (χ_2) at all points in time (solid blue curves above solid red curves for all time points in both panels in the fifth column of Fig. 4). Thus, the relative magnitudes of the sensitivities can be predicted only by knowing which burst size corresponds to which host species.

Note that whether the magnitudes and dynamics of the sensitivities are driven by intraspecific versus interspecific processes, the species' roles, or the species' identities can change over time. This information is useful because it yields insight about how the effects of processes on disease prevalence vary as conditions within the system change.

4.3.1 Analysis of Case 1: Do temporal patterns differ between host species when the pathogen is introduced into the community?

Here we analyze the temporal dynamics of the PRCC sensitivity indices when the pathogen is introduced into a disease-free two-host community. We compare the tem-

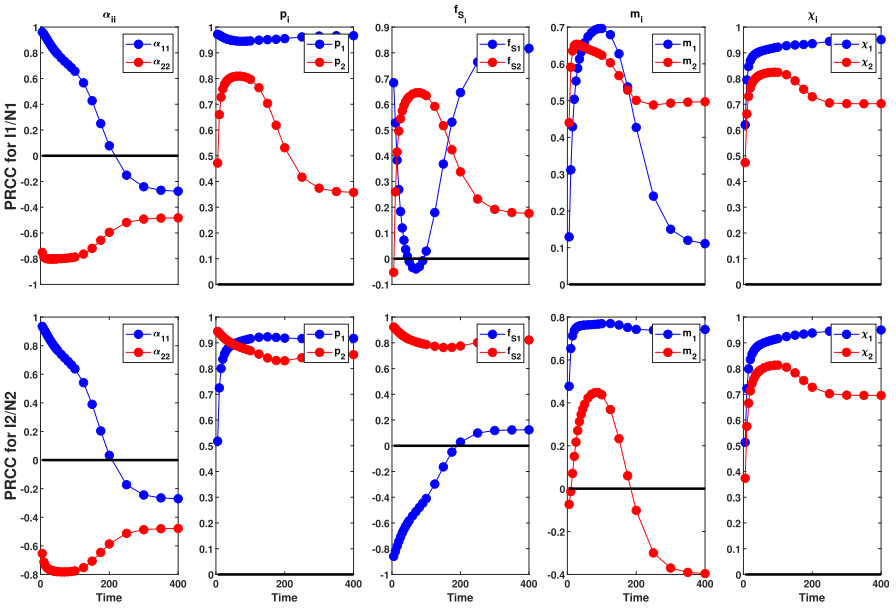

Fig. 4 Comparison of the global sensitivities to all ecological parameters in Case 1. Row 1 shows the sensitivities for disease prevalence in host 1 (I_1/N_1) and row 2 shows the sensitivities for disease prevalence in host 2 (I_2/N_2). In each panel, solid blue circles denote the sensitivity to a parameter for host 1 (e.g., α_{11} or p_1) and the solid red circles denote the sensitivity to a parameter for host 2 (e.g., α_{22} or p_2). The solid black line denotes a PRCC value of 0. When comparing panels in the same column, we say the magnitudes and temporal patterns of the sensitivities are driven by (i) intraspecific vs. interspecific processes if the solid blue curve in the top panel qualitatively matches the solid red curve in the bottom panel and the solid red curve in the top panel qualitatively matches the solid blue curve in the bottom panel or (ii) species' identities if the solid blue curves in the top and bottom panels qualitatively match and the solid red curves in the top and bottom panels qualitatively match. See Sect. 4.3 for additional details (colour figure online)

poral dynamics of the sensitivities for host species 1 (top row in Fig. 4) and host species 2 (bottom row in Fig. 4).

Sensitivities to epidemiological parameters First consider the temporal dynamics of the PRCC values for the most sensitive epidemiological parameters (p_i, f_{S_i}, χ_i, m_i; columns 2–5 in Fig. 4). Early in time (left side of each panel), the magnitudes of the sensitivities are driven by intraspecific versus interspecific processes for p_i, f_{S_i}, and m_i and by the species' identities for χ_i. Specifically, prevalence in each species is more sensitive to the intraspecific probability of infection (p_i; column 2), the intraspecific filtering rate (f_{S_i}; column 3), and the interspecific mortality rate (m_j, $j \neq i$; column 4), but prevalence in both species is more sensitive to the burst size of host 1 (χ_1; column 5). Over time, the sensitivities transition to being driven by intraspecific versus interspecific processes for f_{S_i} and m_i and being driven by species' identities for χ_i and p_i. Specifically, at the end of the simulations (right side of each panel), each host is more sensitive to its own filtering rate (f_{S_i}; column 3) and the mortality rate of the other host (m_j; column 4), and both hosts are more sensitive to the probability of infection for host 1 (p_1; column 2) and the burst size of host 1 (χ_1; column 5). Many of these transitions are non-monotonic, with each parameter having some period of

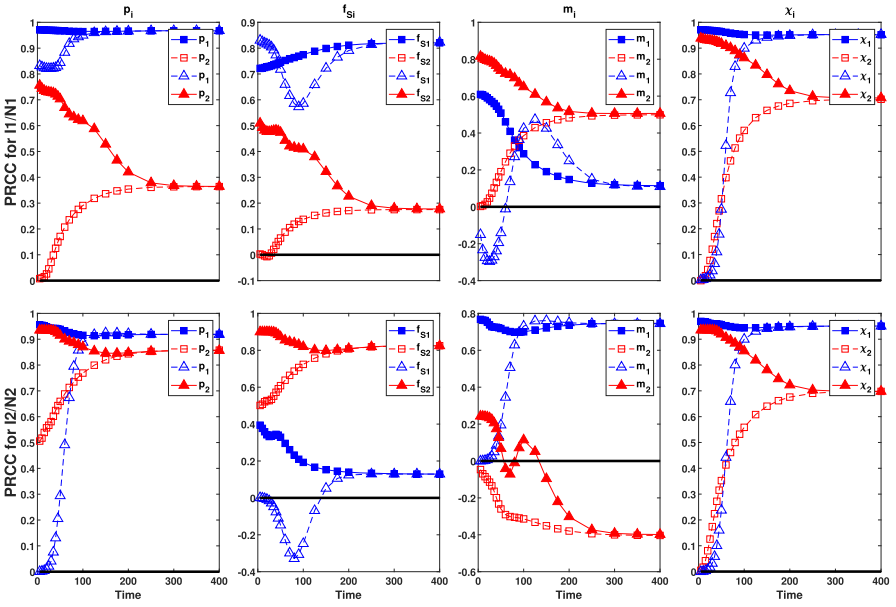

Fig. 5 Comparison of the global sensitivities to all epidemiological parameters in Cases 2 and 3. Row 1 shows the sensitivities for disease prevalence in host 1 (I_1/N_1) and row 2 shows the sensitivities for disease prevalence in host 2 (I_2/N_2). In each panel, blue denotes parameters for host 1, red denotes parameters for host 2, squares denote sensitivities for Case 2, triangles denote sensitivities for Case 3, solid lines with filled symbols denote parameters for the resident host (host 1 in case 2 and host 2 in case 3), and dashed lines with open symbols denote parameters for the invading host (host 2 in case 2 and host 1 in case 3). The solid black line denotes a PRCC value of 0. When comparing panels in the same column, we say the magnitudes and temporal patterns of the sensitivities are driven by (i) intraspecific vs. interspecific processes if the solid blue curve with a filled shape in the top panel qualitatively matches the dashed red curve with the same open shape in the bottom panel, and the dashed blue curve with an open shape in the top panel qualitatively matches the solid red curve with the same filled shape in the bottom panel; (ii) the species' roles of invader vs. resident if the solid blue curve with a filled shape in the top panel qualitatively matches the solid red curve with the same filled shape in the bottom panel, and the dashed blue curve with an open shape in the top panel qualitatively matches the dashed red curve with the same open shape in the bottom panel; and (iii) species' identities if solid curves with filled symbols of one color in the top panel qualitatively match solid curves with filled symbols of the same color in the bottom panel, or if dashed curves with open symbols of one color in the top panel qualitatively match dashed curves with open symbols of the same color in the bottom panel. See Sect. 4.3 for additional details (colour figure online)

time when the relative magnitudes are determined by the species' identify (e.g., both hosts are more sensitive to the filtering rate of host 2 near $t = 200$; red curves are larger in magnitude than blue curves in column 3 of Fig. 4). In addition, prevalence is both species is always more sensitive to χ_1 than χ_2 (blue curves above red curves in column 5).

One biological insight from the above is that host competence is an important quantity to estimate in order to understand how each species will affect the spread of a pathogen across the community. Here, host competence is the ability of a host species to transmit the pathogen to conspecifics and for model (1)–(5) it is $\chi_i\, p_i$ (Cortez 2021). Estimating competence is important because at all time points infection prevalence

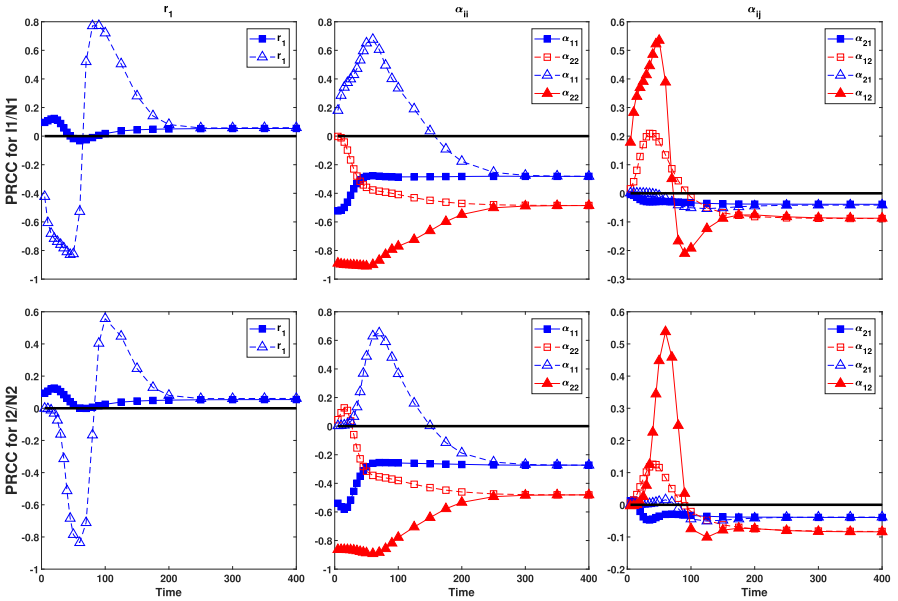

Fig. 6 Comparison of the global sensitivities to all ecological parameters in Cases 2 and 3. Row 1 shows the sensitivities for disease prevalence in host 1 (I_1/N_1) and row 2 shows the sensitivities for disease prevalence in host 2 (I_2/N_2). In each panel, blue denotes parameters for host 1, red denotes parameters for host 2, squares denote sensitivities for Case 2, triangles denote sensitivities for Case 3, solid lines with filled symbols denote parameters for the resident host (host 1 in case 2 and host 2 in case 3), and dashed lines with open symbols denote parameters for the invading host (host 2 in case 2 and host 1 in case 3). The solid black line denotes a PRCC value of 0. When comparing panels in the same column, we say the magnitudes and temporal patterns of the sensitivities are driven by (i) intraspecific vs. interspecific processes if the solid blue curve with a filled shape in the top panel qualitatively matches the dashed red curve with the same open shape in the bottom panel, and the dashed blue curve with an open shape in the top panel qualitatively matches the solid red curve with the same filled shape in the bottom panel; (ii) the species' roles of invader vs. resident if the solid blue curve with a filled shape in the top panel qualitatively matches the solid red curve with the same filled shape in the bottom panel, and the dashed blue curve with an open shape in the top panel qualitatively matches the dashed red curve with the same open shape in the bottom panel; and (iii) species' identities if solid curves with filled symbols of one color in the top panel qualitatively match solid curves with filled symbols of the same color in the bottom panel, or if dashed curves with open symbols of one color in the top panel qualitatively match dashed curves with open symbols of the same color in the bottom panel. See Sect. 4.3 for additional details (colour figure online)

is highly sensitive to the spore burst sizes (χ_i) and infection probabilities (p_i) of both species. A second biological insight is that species removal can have counter-intuitive effects on infection prevalence. Specifically, increased mortality of host 1 (m_1) increases infection prevalence in both species at all time points (blue circles in column 4 of Fig. 4). Increased mortality of host 2 (m_2) also increases host 1 infection prevalence at all points in time and it increases host 2 infection prevalence at intermediate time scales (red circles in column 4). These counter-intuitive responses are due to the host shedding rates ($\chi_i m_i$) being products of their burst sizes and mortality rates. Our results suggest that removal-based disease control measures (e.g., increased mortality

caused by culling) potentially can be counterproductive and lead to increased levels of disease in one or both species.

Sensitivities to ecological parameters Now consider the temporal dynamics of the PRCC values for the most sensitive ecological parameters (α_{ii}; column 1 of Fig. 4). The dynamics of the sensitivities are predicted by host identity. In particular, the sensitivities to the competition parameter for host 1 (α_{11}) monotonically decrease from large positive values to small negative values (blue curves in column 1 of Fig. 4). In comparison, the sensitivities to the competition parameter for host 2 (α_{22}) are negative for all time, but transiently increase in magnitude before ultimately decreasing in magnitude (red curves in column 1 of Fig. 4). This contrasting pattern is due to host 2 having higher competence than host 1 (i.e., $\chi_2 p_2 > \chi_1 p_1$). Specifically, slower growth of host 2 (larger α_{22}) and faster growth of host 1 (smaller α_{22}) both cause slower increases in spore density, which leads to fewer infections in both host species.

A biological insight from the above is that accurate prediction of the effects of host densities on outbreak dynamics early in time requires accurate knowledge about host competence. Early in time, the total density for each species is primarily determined by the intraspecific competition coefficients (α_{11}, α_{22}). Because the effects of reduced host density (i.e., higher α_{ii}) are driven by species identity, predicting whether the reduced density of host i increases or decreases infection prevalence in both host species at short time scales requires accurate knowledge about host competence.

4.3.2 Analysis of Cases 2 and 3: How do temporal patterns depend on which host species is the resident versus invader?

Here we focus on similarities and differences in the temporal dynamics of the PRCC values when one host species is the resident and the other host species is the invader. We focus on (i) comparing the temporal dynamics of the sensitivities for the invading species (solid curves with filled symbols in Figs. 5 and 6) and (ii) comparing the temporal dynamics of the sensitivities for the resident species (dashed curves with open symbols in Figs. 5 and 6).

Sensitivities to epidemiological parameters First consider the temporal dynamics of the PRCC values for the most sensitive epidemiological parameters (p_i, f_{S_i}, χ_i, m_i); see Fig. 5. Early in time in both cases 2 and 3, the species' roles (i.e., invader versus resident) determine if prevalence in each species is more sensitive to the resident's or invader's parameters. Specifically, both hosts are more sensitive to the resident's epidemiological parameters than the invader's parameters (solid curve larger in magnitude than dashed curves early in time in Fig. 5); the only exception is that the invading host is more sensitive to its filtering rate (f_{S_i}) than the filtering rate of the resident host species (blue curves above red curves in top panel of column 2 in Fig. 5 and red curves above blue curves in bottom panel of column 2). Over time, the sensitivities transition to being predicted by intraspecific versus interspecific processes for f_{S_i} and m_i and being predicted by species' identities for χ_i and p_i. Many of these transitions are monotonic (e.g., columns 1 and 4 in Fig. 5), however non-monotonic changes occur for the filtering rates (f_{S_i}; column 2 of Fig. 5) and mortality rates (m_i; column 3 in Fig. 5).

Sensitivities to ecological parameters Now consider the temporal dynamics of the PRCC values for the most sensitive ecological parameters (α_{ij}, r_i); see Fig. 6. Early in time in both cases 2 and 3, the species' roles (i.e., invader versus resident) determine if prevalence in each species is more sensitive to the resident's or invader's parameters. Specifically, both hosts are more sensitive to the resident's competition parameters than the invader's (solid curves with filled symbols are larger in magnitude than dashed curves with the same open symbol and the opposite color early in time in Fig. 6). Later in time, the magnitudes of the sensitivities are driven by the species' identities. When host 1 is the resident (Case 2), the sensitivities for all competition parameters are below the 0.6 threshold for all time (all curves with squares in Fig. 6 are less than 0.6 in magnitude for all time). In comparison, when host 2 is the resident (Case 3), the sensitivities to the exponential growth rate of host 1 (r_1) and both intraspecific competition parameters (α_{11}, α_{22}) are above the threshold for some period of time (curves with triangles in columns 1 and 2 of Fig. 6 are greater than 0.6 in magnitude). In addition, the sensitivities to the interspecific competition parameters (α_{12}, α_{21}) are often larger in Case 3 than Case 2 (curves with triangles are typically greater in magnitude than curves with squares in column 3 of Fig. 6). Interestingly, this pattern is the opposite of what one might expect given that host 2 is the stronger intraspecific and interspecific competitor (α_{i2} larger than α_{i1}). We suspect that it is due to host 2 being at lower densities than host 1, which results in competition having a relatively larger effect on the disease dynamics of the system.

Combined, the above yields two pieces of biological insight. First, our results suggest that it is more important to accurately estimate the ecological and epidemiological trait values for resident host species than invading host species in order to accurately predict the short-term dynamics immediately after an invasion. This is because the dynamics are more sensitive to the resident's trait values early in time. Second, our results suggest accurate prediction of the long-term dynamics after an invasion is likely to require accurate estimates of both the resident's and the invader's epidemiological trait values. This is because at longer time scales the dynamics can be highly sensitive to both the resident's and invader's epidemiological trait values.

5 Discussion and conclusions

In this study we used global sensitivity analysis to gain insight into how ecological and epidemiological processes shape the temporal dynamics of a two-host-one-pathogen community. This study demonstrates that the temporal patterns of the sensitivities can yield insight into how specific processes are affecting quantities of interest at different points in time. In particular, comparing the temporal dynamics of the sensitivities of the two host species identifies when the effects of a process are driven by the specific characteristics of each species (i.e., species' identities) versus properties of the system that are independent of the species' identities (i.e., intraspecific versus interspecific processes and the species' roles of invader versus resident). Biologically, this is useful because it helps determine what information is needed to make predictions about how a specific process shapes disease dynamics. For example, when a pathogen is introduced into a disease-free community (Case 1), one must know the competitive

abilities of each host species (e.g., α_{ij}) in order to predict how host competition affects disease dynamics at all points time. In contrast, when a second host is introduced into an endemic single-host community, only knowledge of the competitive ability of the resident host is needed to predict how host competition affects disease dynamics over short time scales.

Sensitivity analysis can also help one predict if the dynamics of the system are likely to be altered by temporal changes in the signs of the effects of specific processes. If a quantity of interest is weakly sensitive to a specific parameter or process, then sign changes in the sensitivity for that parameter are less likely to have a measurable effect on the system dynamics. More generally, ranking the sensitivities of all parameters allows one to identify the most sensitive parameters and reduce the number of parameters that need to be considered. For example, in Cases 2 and 3, the sensitivity of prevalence in host 1 (N_1/I_1) to host 2's filtering rate (f_{S_2}) is below our threshold for all points in time (red curves below 0.6 in top panel of column 2 of Fig. 5). If the goal is to predict how host 2 affects host 1 infection prevalence, then host 2's filtering rate is less important to accurately measure than host 2's shedding rate (χ_2), whose sensitivities are above the threshold for sufficiently large time points (red curves above 0.6 in top panel of column 4 of Fig. 6).

5.1 Implications for host species richness-disease relationships

Many prior studies have argued that the relationships species richness (i.e., the number of host species) and disease levels in a focal host are likely to be context dependent (Halliday et al. 2020; LoGiudice et al. 2008; Randolph and Dobson 2012; Rohr et al. 2020). This is supported by previous empirical studies (Dizney and Ruedas 2009; Hydeman et al. 2017; Levine et al. 2017; Luis et al. 2018; Searle et al. 2016; Telfer et al. 2005; Zimmermann et al. 2017) and theoretical studies (Cortez and Duffy 2021; Cortez 2021; Dobson 2004; Faust et al. 2017; Joseph et al. 2013; Mihaljevic et al. 2014; O'Regan et al. 2015; Roberts and Heesterbeek 2018; Rudolf and Antonovics 2005; Searle et al. 2016) showing that the effects of host additions on focal host disease levels depend on the specific characteristics of the host species (e.g., competitive ability and disease competence) that are present in the community and added to the community. The global sensitivity results in this study suggest that the context dependent relationships also depends on the time scale of interest. Thus, addition of a host species could initially decrease disease, but ultimately increase disease.

One particular example of this issue is the interpretation of short-term exposure experiments. Prior empirical studies (Becker et al. 2014; Evans and Entwistle 1987; Hopkins et al. 2020; Johnson et al. 2008; Orlofske et al. 2012; Searle et al. 2011; Venesky et al. 2014) have used short-term exposure experiments to infer how the presence or absence of alternative host species affect disease levels in a focal host species. The intuition is that higher (lower) prevalence in a short term experiment will translate to higher (lower) prevalence over the long term. The sensitivities for the host filtering rates (f_{S_i}) in Case 1 suggest that this intuition may be incorrect. Specifically, introduction of a host with a higher filtering rate could lead to lower infection prevalence over the short term (because the sensitivity of I_i/N_i to f_{S_j} for

$i \neq j$ is negative for small t) but positive over the long term (because the sensitivity of I_i/N_i to f_{S_j} for $i \neq j$ is positive for small t); see Table 2. The difference arises because the short-term dynamics do not account for indirect effects between species that become larger in magnitude over time. In particular, increased uptake leads to more infections in host j, which leads to greater release of spores by infected individuals of host j and ultimately increased infection rates in host i. Our results also show that for some processes the effects on disease prevalence have effects of constant sign. For example, increased burst sizes for either host (larger χ_i) has a positive effect on disease prevalence in both host species at all time points. Thus, while our results suggest caution when making inferences about long term disease levels from short-term experiments, they also illustrate that global sensitivity analysis can be used to make predictions about when processes may potentially have effects of different signs on system dynamics.

5.2 Directions of future work

This study has focused on applying global sensitivity analysis to a specific region of parameter space in order to study the effects of ecological and epidemiological processes on a particular disease metric (infection prevalence). Previous studies (Cortez and Duffy 2021; Cortez 2021; Roberts and Heesterbeek 2018) have shown that the signs of local sensitivities at equilibrium can differ across parameter space. Exploring how the temporal patterns of the sensitivities vary across parameter space is likely to yield insight about if and when patterns can be generally explained by the species' identities or by other factors (e.g., invader versus resident or intraspecific versus interspecific processes). In addition, prior studies (Cortez and Duffy 2021; Roche et al. 2012; Roberts and Heesterbeek 2018) have shown that predictions from local sensitivities can differ depending on whether the metric of disease is infection prevalence, infected density, or pathogen's basic reproduction number ($\mathcal{R}_0$). Applying global sensitivity analysis to other metrics could yield insight into why those metrics respond differently to ecological and epidemiological processes and how that depends on the time scale of interest. Furthermore, by partitioning into different kinds of ecological and epidemiological processes, global sensitivity analysis may also yield additional insight about how other kinds of interspecific interactions between species in a community (e.g., predation) affect disease dynamics.

Additional insight also could be gained by using alternative global sensitivity measures. One alternative is Sobol' sensitivity indices, where the first order Sobol' index (S_i) estimates the reduction in variance in the quantity of interest that occurs when parameter q_i is held fixed. We estimated the Sobol' first order indices for the quantities of interest and region of parameter space analyzed in this study and found that $\sum_i S_i \approx 1$ (by definition $\sum_i S_i \leq 1$). This suggests that higher order interactions between parameters only have small effects on the quantities of interest. Because PRCC and Sobol' first order indices provide similar parameter rankings, our results from the Sobol' sensitivity indices suggest that the PRCC indices are sufficient to explore the dynamics of the system completely. However, in systems where $\sum_i S_i \ll 1$ (e.g., the epidemiological system in Hanthanan Arachchilage and Hussaini (2021)),

higher order sensitivity indices can provide new insight into how interactions between processes influence system behavior.

Other alternatives that can be used with correlated parameters such as moment independent measures such as those in Kucherenko et al. (2012), Xu et al. (2022) and Mara and Tarantola (2012). PRCC and Sobol' sensitivity indices assume that the input parameters, q_i, are statistically uncorrelated, but correlations between parameters can arise in many systems. For example, in this system susceptible individual filtering rates, infected individual filtering rates, and the competition coefficients are all likely to be positively correlated. Approaches based on moment independent measures can account for correlated parameters, and those approaches may yield additional insight about the sensitivities to specific processes and the relationships between first and higher order indices.

In closing, this study illustrates how GSA methodology can provide useful insight into the ecological and epidemiological processes that are modeled using mathematics. Understanding the details of specific quantities of interest, time-evolution, and interpretation of the GSA rankings requires an understanding of the underlying mathematics, modeling, and biology, and the synthesis provides more information than each aspect alone.

Supplementary Information The online version contains supplementary material available at https://doi.org/10.1007/s00285-023-01912-w.

Acknowledgements MHC was supported by the National Science Foundation under Award DEB-2015280. The authors thank three anonymous reviewers for comments that helped improve the manuscript.

Author Contributions All authors designed the study. KHA did all numerical calculations. All authors wrote and edited the manuscript.

Data availability statement Data sharing not applicable to this article as no datasets were generated or analysed during the current study.

Declarations

Conflict of interest The authors have no relevant financial or non-financial interests to disclose

References

Becker CG, Rodriguez D, Toledo LF, Longo AV, Lambertini C, Corrêa DT, Leite DS, Haddad CF, Zamudio KR (2014) Partitioning the net effect of host diversity on an emerging amphibian pathogen. Proc R Soc B Biol Sci 281:20141796

Blower SM, Dowlatabadi H (1994) Sensitivity and uncertainty analysis of complex models of disease transmission: an hiv model, as an example. International Statistical Review/Revue Internationale de Statistique, pp 229–243

Cortez MH (2021) Using sensitivity analysis to identify factors promoting higher versus lower infection prevalence in multi-host communities. J Theor Biol 526:110766

Cortez MH, Duffy MA (2021) The context-dependent effects of host competence, competition, and pathogen transmission mode on disease prevalence. The American Naturalist 198

Dizney LJ, Ruedas LA (2009) Increased host species diversity and decreased prevalence of Sin Nombre Virus. Emerg Infect Dis 15:1012–1018

Dobson A (2004) Population dynamics of pathogens with multiple host species. Am Nat 164:S64–S78

Evans HF, Entwistle PF (1987) Viral diseases. In: Fuxa JR, Tanada T (eds) Epizootiology of insect diseases. Wiley, New York

Faust CL, Dobson AP, Gottdenker N, Bloomfield LS, McCallum HI, Gillespie TR, Diuk-Wasser M, Plowright RK (2017) Null expectations for disease dynamics in shrinking habitat: Dilution or amplification? Philos Trans R Soc B Biol Sci 372:20160173

Halliday FW, Rohr JR, Laine A-L (2020) Biodiversity loss underlies the dilution effect of biodiversity. Ecol Lett 23:1611–1622

Hamby D (1995) A comparison of sensitivity analysis techniques. Health Phys 68:195–204

Hanthanan Arachchilage K, Hussaini M (2021) Ranking non-pharmaceutical interventions against covid-19 global pandemic using global sensitivity analysis-effect on number of deaths. Chaos Solitons Fractals 152:111458

Hopkins SR, Fleming-Davies AE, Belden LK, Wojdak JM (2020) Systematic review of modelling assumptions and empirical evidence: Does parasite transmission increase nonlinearly with host density? Methods Ecol Evol 11:476–486

Hydeman ME, Longo AV, Velo-Antón G, Rodriguez D, Zamudio KR, Bell RC (2017) Prevalence and genetic diversity of batrachochytrium dendrobatidis in Central African island and continental amphibian communities. Ecol Evol 7:7729–7738

Jansen M (1999) Analysis of variance designs for model output. Comput Phys Commun

Jarrett A, Cogan N, Hussaini M (2017) Combining two methods of global sensitivity analysis to investigate mrsa nasal carriage model. Bull Math Biol 79:2258–2272

Jarrett AM, Cogan N, Hussaini M (2017) Combining two methods of global sensitivity analysis to investigate mrsa nasal carriage model. Bull Math Biol 79:2258–2272

Johnson PT, Hartson RB, Larson DJ, Sutherland DR (2008) Diversity and disease: community structure drives parasite transmission and host fitness. Ecol Lett 11:1017–1026

Joseph MB, Mihaljevic JR, Orlofske SA, Paull SH (2013) Does life history mediate changing disease risk when communities disassemble? Ecol Lett 16:1405–1412

Kucherenko S, Tarantola S, Annoni P (2012) Estimation of global sensitivity indices for models with dependent variables. Comput Phys Commun 183:937–946

Levine RS, Hedeen DL, Hedeen MW, Hamer GL, Mead DG, Kitron UD (2017) Avian species diversity and transmission of west nile virus in Atlanta, Georgia. Parasites Vect 10:62

LoGiudice K, Duerr ST, Newhouse MJ, Schmidt KA, Killilea ME, Ostfeld RS (2008) Impact of host community composition on lyme disease risk. Ecology 89:2841–2849

Luis AD, Kuenzi AJ, Mills JN (2018) Species diversity concurrently dilutes and amplifies transmission in a zoonotic host-pathogen system through competing mechanisms. Proc Natl Acad Sci 115:7979–7984

Mara T, Tarantola S (2012) Variance-based sensitivity indices for models with dependent inputs. Reliab Eng Syst Saf 107:115–121

Marino S, Hogue I, Ray C, Kirschner D (2008) A methodology for performing global uncertainty and sensitivity analysis in systems biology. J Theor Biol 254:178–196

Mihaljevic JR, Joseph MB, Orlofske SA, Paull SH (2014) The scaling of host density with richness affects the direction, shape, and detectability of diversity-disease relationships. PLoS ONE 9:e97812

O'Regan SM, Vinson JE, Park AW (2015) Interspecific contact and competition may affect the strength and direction of disease-diversity relationships for directly transmitted microparasites. Am Nat 186:480–494

Orlofske SA, Jadin RC, Preston DL, Johnson PT (2012) Parasite transmission in complex communities: predators and alternative hosts alter pathogenic infections in amphibians. Ecology 93:1247–1253

Randolph SE, Dobson ADM (2012) Pangloss revisited: a critique of the dilution effect and the biodiversity-buffers-disease paradigm. Parasitology 139:847–863

Roberts M, Heesterbeek J (2018) Quantifying the dilution effect for models in ecological epidemiology. J R Soc Interface 15:20170791

Roche B, Dobson AP, Guegan JF, Rohani P (2012) Linking community and disease ecology: the impact of biodiversity on pathogen transmission. Philos Trans R Soc B 367:2807–2813

Rohr JR, Civitello DJ, Halliday FW, Hudson PJ, Lafferty KD, Wood CL, Mordecai EA (2020) Towards common ground in the biodiversity-disease debate. Nat Ecol Evol 4:24–33

Rudolf VHW, Antonovics J (2005) Species coexistence and pathogens with frequency-dependent transmission. Am Nat 166:112–118

Salelli A, Tarantola S, Campolongo F, Ratto M (2004) Sensitivity Analysis in Practice, a guide to assessing scientific models. Wiley

Saltelli A, Aleksankina K, Becker W, Fennell P, Ferretti F, Holst N, Li S, Wu Q (2019) Why so many published sensitivity analyses are false: a systematic review of sensitivity analysis practices. Environ Model Softw 114:29–39

Searle CL, Biga LM, Spatafora JW, Blaustein AR (2011) A dilution effect in the emerging amphibian pathogen Batrachochytrium dendrobatidis. Proc Natl Acad Sci 108:16322–16326

Searle CL, Cortez MH, Hunsberger KK, Grippi DC, Oleksy IA, Shaw CL, de la Serna SB, Lash CL, Dhir KL, Duffy MA (2016) Population density, not host competence, drives patterns of disease in an invaded community. Am Nat 188:554–566

Sobol I (2001) Global sensitivity indices for nonlinear mathematical models and their monte carlo estimates. Math Comput Simul 55:271–280

Telfer S, Bown K, Sekules R, Begon M, Hayden T, Birtles R (2005) Disruption of a host-parasite system following the introduction of an exotic host species. Parasitology 130:661

Venesky MD, Liu X, Sauer EL, Rohr JR (2014) Linking manipulative experiments to field data to test the dilution effect. J Anim Ecol 83:557–565

Wentworth M, Smith R, Banks H (2016) Parameter selection and verification techniques based on global sensitivity analysis illustrated for an hiv model. SIAM/ASA J Uncertain Quant 4:266–297

Xu G, Hanthanan Arachchilage K, Hussaini M, Oates W (2022) Quantifying the uncertainty and global sensitivity of quantum computations on experimental hardware. Quant Inf Process 21:1–38

Zimmermann MR, Luth KE, Esch GW (2017) Snail species diversity impacts the infection patterns of echinostoma spp.: examples from field collected data. Acta Parasitol 62:493–501